Failure at Reinforced Sections of Spherical Steel Containments Under Excessive Internal Pressure

B. Göller, R. Krieg, G. Messemer

Kernforschungszentrum Karlsruhe GmbH, Institut für Reaktorentwicklung, Projekt Nukleare Sicherheit, Postfach 3640, D-7500 Karlsruhe 1, Germany

Summary

In case of a hypothetical core melt accident the pressure inside the containment is expected to grow beyond the design limit up to containment failure, which may occur in the containment shell close to reinforced sections, where large plastic strains are concentrated. Experimental and theoretical investigations have been performed in order to study the behaviour of the containment under these conditions. It turned out that failure occurs due to plastic instability with a crack running round the reinforcement. Furthermore the failure pressure is only slightly influenced by the type of the reinforcement.

1. Introduction

In case of a hypothetical core melt accident the pressure inside the containment is expected to grow beyond the design limit up to containment failure /1, 2/, which then will occur at the weakest containment part. This might be the containment shell close to reinforced sections which surround nozzles, locks and other penetrations. In these regions the smooth state of stresses and strains occuring in a perfect spherical shell is disturbed what induces a local increase in stresses and strains. Thus, for growing pressure, the containment might fail in these regions. The failure pressure and the failure mode are investigated in this paper.

Of course, there are other weak parts in the containment which may have a lower failure pressure. These parts will be investigated separately.

2. Computational Model

The theoretical investigation of the containment in the neighbourhood of reinforced sections is based on the computer program ROTMEM /3/. It allows for calculation of the membrane stresses and strains of an axisymmetric shell under axisymmetric pressure loading. Any elastic-plastic material behaviour can be considered. Large deformations including changes of wall thickness are taken into account. However, bending and shear stresses are neglected. The conditions of equilibrium for an axisymmetric membrane are:

$$p = \frac{N_\varphi}{r_\varphi} + \frac{N_\theta}{r_\theta} \; ; \quad p_\varphi = (N_\theta - N_\varphi) \cdot \frac{\cot \varphi}{r_\theta} - \frac{\partial N_\varphi}{r_\varphi \partial \varphi} \qquad (1)$$

N_φ and N_θ are the stress resultants, r_φ and r_θ are the principal radii of curvature, p and p_f are the pressure loadings and φ and θ are meridional and circumferential coordinates. For the numerical treatment the membrane is described by the coordinates of discrete points of a meridian. The radii of curvature, the tangent angle φ and the strains of the membrane can easily be determined from these data. Using the deviatoric strains e_i the deviatoric stresses s_i can be computed by inverting the Prandtl-Reuss equation

$$d e_i = \frac{1}{2G} \cdot d s_i + s_i \, d\lambda \qquad (2)$$

G is the shear modulus, and $d\lambda$ is the strain hardening parameter which may be derived from an uniaxial tensile test of the material. From the stresses s_i the stress resultants N_φ and N_θ can be determined. Thus, from the conditions of equilibrium (1) that loading can be computed which is required to keep the membrane in its actual deformation state. If these values agree with the given loading, the solution is found. Otherwise the geometric configuration will be changed iteratively by the Newton-Raphson-method such that the calculated loading approaches the given loading.

In computations for membranes with reinforcements typical for containments very sharp strain peaks occurred in front of the reinforcement, leading to unrealistic sharp necking regions. It turned out that this behaviour was due to the neglect of transverse stresses. Analysis of the three-dimensional state of stresses in the necking region yields the mean value of the normal stress, averaged over the membrane thickness:

$$\sigma_n = \frac{1}{6} \cdot N_\varphi \cdot \varkappa_h \qquad (3)$$

where $\varkappa_h$ is the curvature of the necking surface of the membrane. The influence of this normal stress was taken into account in the stress-strain relation (2) for an improved version of ROTMEM. In this way a certain smoothening of the necking region was obtained.

3. Experimental Investigations

Experiments on containment models with excessive internal pressure have been found to be unsuitable, since manufacture of several models in correct scale (thin spherical shells) would be very expensive. Instead tests with initially plane circular membranes loaded by unilateral liquid pressure up to failure have been done. The membranes have been manufactured by facing thicker plates with a lathe. The plates used for this process were the same as those used for PWR-containments (15MnNi63-sheets with a thickness of 38 mm). The diameter of the membranes is 860 mm, the thickness is 2 mm. Some membranes are smooth, others contain reinforced sections.

During the test the pressure is increased in steps of about 5 bar until failure. After each step the displacements of a large number of control points marked on the membrane are measured using a three-coordinate measuring machine (Fig. 1). For the same points also the decreasing thickness of the membrane is determined using an ultrasonic sensor.

Based on these data, the three components of strain have been computed. The stresses in the membrane can be determined from the conditions of equilibrium, with the radii of curvature determined from the coordinates of the measured control points. Thus, the stress-strain-

relation for a two-axial state of stresses could be determined and the validity of the v. Mises stress hypothesis could be checked /4/.

Two membranes with a constant wall-thickness of 2 mm were tested first. Both membranes failed at a pressure of 43 bar with a central deflection of 250 mm (Fig. 2). The wall thickness had decreased to 1.2 mm. The equivalent strains were rather high with values of 50 % (in-plane strain component 25 %).

Failure of both membranes was controled by plastic instability. This means, that a deformation state of the system is reached at which additional deformations cause a large reduction in wall thickness which cannot be compensated by the strain hardening of the material. Fig. 3 shows the decrease of the wall thickness as a function of the increasing pressure. Computation and experiment agree quite well. The computations indicate plastic instability at a pressure of 45.2 bar. As mentioned above the actual failure pressure was 43 bar.

Additionally two membranes were tested which had a circular reinforcement at its center (diameter 132 mm, thickness 3.4 mm, the other dimensions being the same as before). Now the membranes failed at pressures of 28 and 32 bar, respectively, what is considerably lower than the failure pressure of 43 bar for the membranes without reinforcement. The central deflections now were 113 mm and 132 mm, and the wall thicknesses had decreased to 1.68 mm and 1.61 mm, respectively. The equivalent strains in the failed region were only 16 % and 22 %, respectively. The failed membranes had a crack running approximately 2 mm in front of the reinforcement (Fig. 4). This can be explained by the large plastic strains which are concentrated in a very small region around the reinforcement (Fig. 5).

The differences between the experimental results for both membranes - which ought to be manufactured identical - indicate that this system is very sensitive to small (manufacturing) parameter variations. This was confirmed by several computations, in which a smoothening of the transition region to the reinforced section has increased the failure pressure significantly. Taking into account such a smoothening and applying the improved version of ROTMEM, good agreement between measured and computed wall thicknesses up to a pressure of 25 bar has been obtained (Fig. 6). For the point of failure, it should be mentioned, that the lowest wall thickness of 1.2 mm has not been measured at the pressurized membrane, but after failure by plastic instability.

Fortunately, the computations for the spherical containment (next section) will show that this system is less sensitive in this respect.

4. Results for the Containment

In order to investigate failure of the containment due to internal overpressurization the program ROTMEM has been applied. As only axisymmetric problems can be analysed, it is necessary to move the reinforcement to the pole of the containment. The dimensions used for the calculaltions are shown in Fig. 7. During core-melt accident a temperature of 170 ^{o}C is expected to occur in the containment wall /1/; thus the material properties of the containment steel (15MnNi63) at this temperature have been used (Fig. 8). At the elevated temperature the yield stress is reduced, while the ultimate tensile stress is increased.

Up to an internal pressure of 9 bar the material is still linear elastic and the strains in the containment are rather smoothly distributed (Fig. 9a). Especially there are no significant strain peaks near the reinforcement. Global equivalent membrane strains at this pres-

sure are 0.18 %, the maximum displacement (at the pole) is 37 mm.

With increasing pressure the yield stress is first exceeded in front of the reinforcement, while the reinforcement itself remains still elastic. Thus large concentrations of strain occur in front of the reinforcement, as shown in Fig. 9b for a pressure of 9.5 bar. Global equivalent strains are 1 %, the maximum local strain is 1.4 % and the largest displacement (at the pole) is 160 mm.

Fig. 9c shows the strains in the containment for a pressure of 14.25 bar, where the largest displacement has just reached a value of 1 m. Global strains then are in the order of 6 %. The reinforcement has undergone plastic deformations too, in the order of 2 %.

Fig. 10 shows the maximum equivalent strains versus pressure occuring in front of the reinforcement. In order to study the sensitivity of the containment with respect to different types of reinforcements, additional cases, mentioned in Fig. 10, have been investigated. It is very interesting to see, that for all these cases plastic instability occurs at nearly the same pressure of 15.4 bar. The size of the reinforcement, or wheather there is a reinforcement at all, is only of minor importance for the failure pressure. Furthermore, the strain increase close to plastic instability is very strong. Therefore any material defect reducing the ultimate strain to 10 %, for instance, has little influence on the failure pressure.

However, once failure has occured the crack will quickly propagate around the reinforcement, what has been demonstrated during the membrane tests (Fig. 4). This causes a hole in the containment and consequently strains more than twice as high as before must be endured (case P5 in Fig. 10). Furthermore, the maximum pressure which the damaged structure can withstand is slightly lower than the pressure reached before. As a result large cracks are expected to propagate in radial direction leading to global failure of the containment.

As mentioned before, however, this type of failure could only occur, if there would be no weaker parts in the containment. Therefore final conclusions can be drawn only after the failure pressures of other weak parts have been investigated.

5. References

/ 1 / Gesellschaft für Reaktorsicherheit, "Deutsche Risikostudie Kernkraftwerke", Fachband 5: Untersuchung von Kernschmelzunfällen, TÜV Rheinland GmbH, 1980

/ 2 / HOSEMANN, J.P., "On the Fission Product Relase into the Environment during a PWR Core Meltdown Accident", Tenth Water Reactor Research Inf. Meeting, Gaitherburg, Oct. 15, 1982

/ 3 / GÖLLER, B., "Zum Verhalten eines DWR-Containments unter hohem, quasistatischem Innendruck - Grundlagen des Programmes ROTMEM", Internal Report

/ 4 / KRIEG, R., EBERLE, F., GÖLLER, B., GULDEN, W., KADLEC, J., MESSEMER, G., and WOLF, E., "Spherical Steel Containments of Pressurized Water Reactors under Accident Conditions - Investigation program and first results", Nucl. Eng. Design 82, 77-78 (1984)

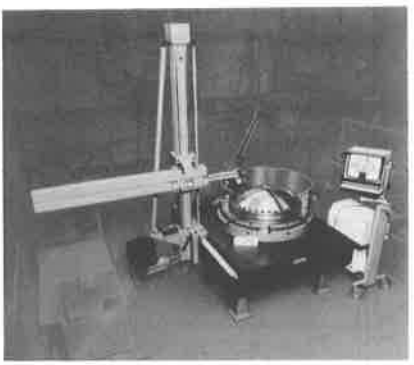

Fig. 1: Three–coordinate measuring machine

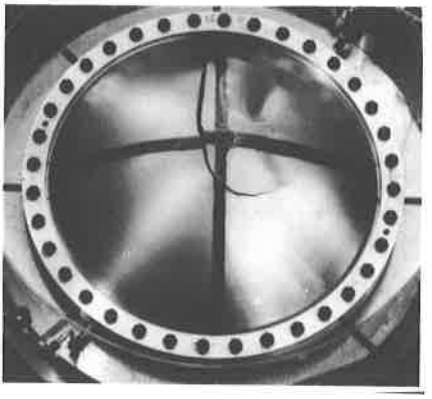

Fig. 2: Membrane with constant wallthickness, failed at 43 bar.

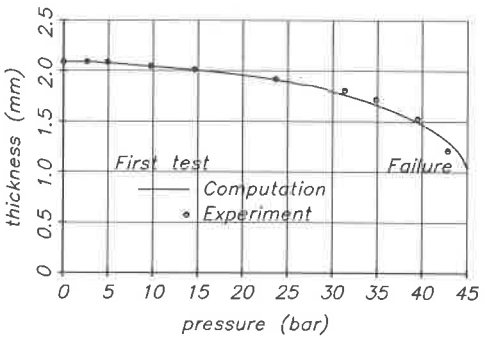

Fig. 3: Membrane with constant wallthickness

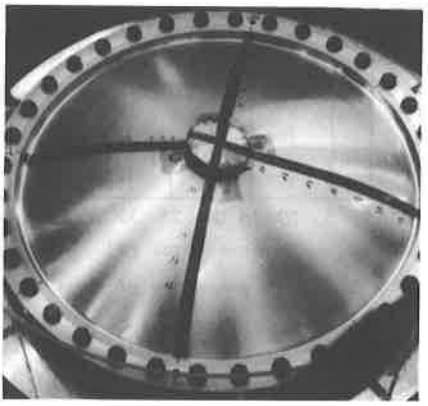

Fig. 4: Membrane with reinforcement, failed at 28 bar.

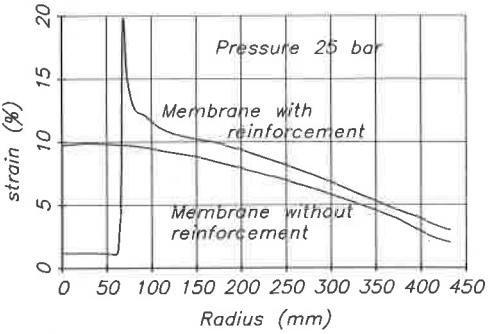

Fig. 5: Equivalent Strains in membranes with and without reinforcement.

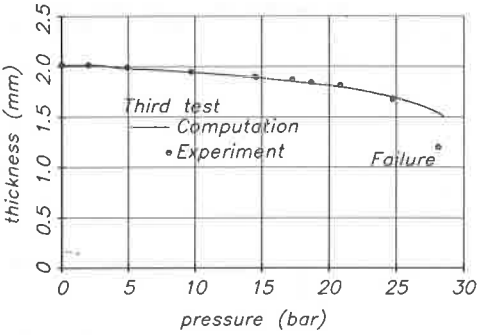

Fig. 6: Membrane with reinforcement

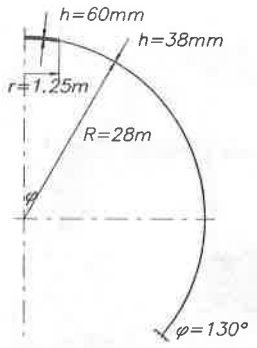

Fig. 7: Containment model with reinforcement

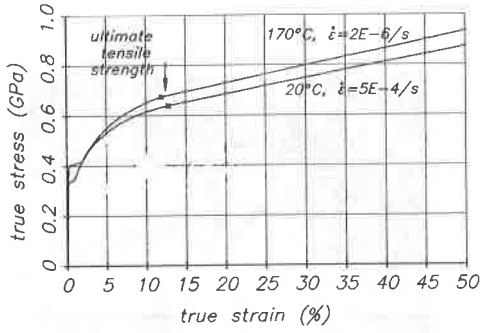

Fig. 8: Measured properties of steel 15MnNi63.

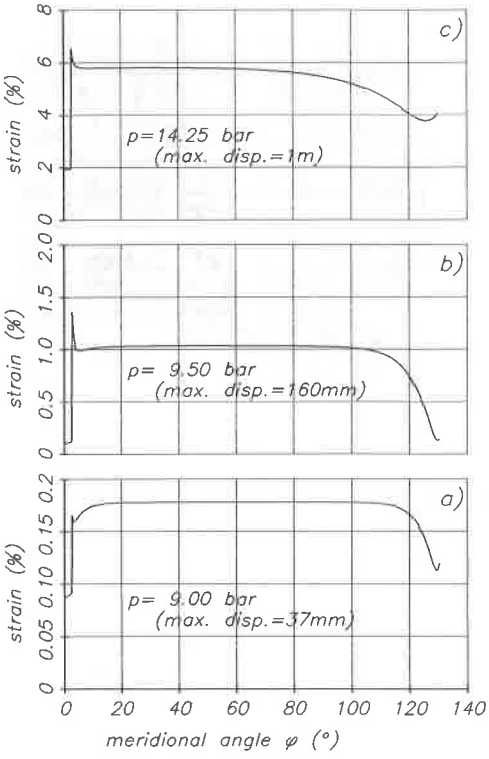

Fig. 9: Equivalent strains in the containment for different pressures

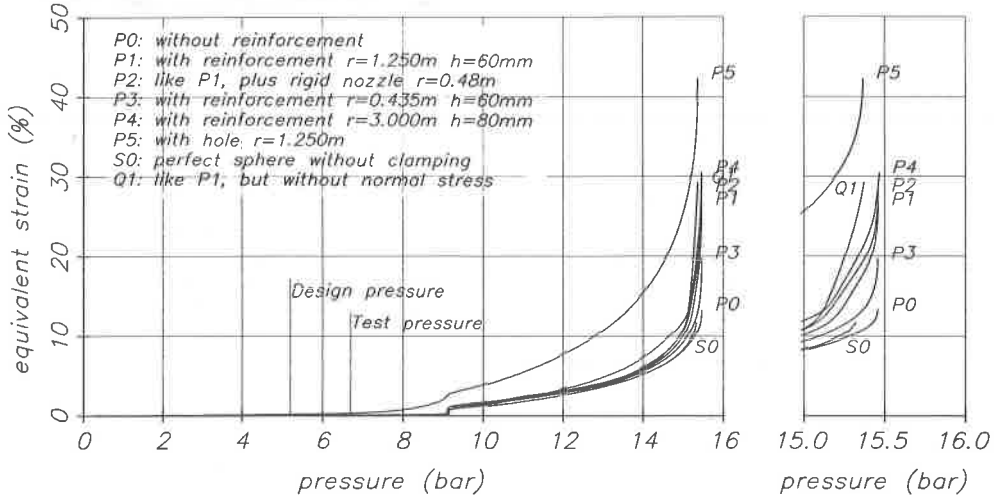

Fig. 10: Maximum strains in the containment for different reinforcements.